Journal of Inorganic Biochemistry 199 (2019) 110791

Contents lists available at ScienceDirect

Journal of Inorganic Biochemistry

journal homepage: www.elsevier.com/locate/jinorgbio

# Ag(I) camphor complexes: antimicrobial activity by design

M. Fernanda N.N. Carvalho[a,*], Silvestre Leite[a,b], Joana P. Costa[a], Adelino M. Galvão[a], Jorge H. Leitão[b,*]

[a] Centro de Química Estrutural, Instituto Superior Técnico, Universidade de Lisboa, Av. Rovisco Pais, 1049-001 Lisboa, Portugal
[b] Instituto de Bioengenharia e Biociências, Departamento de Bioengenharia, Instituto Superior Técnico Universidade de Lisboa, Av. Rovisco Pais, 1049-001 Lisboa, Portugal

ARTICLE INFO

*Keywords:*
Antibacterials
Silver complexes
Camphorimines
Gram-positive bacteria
Gram-negative bacteria
Structure-activity relationships

ABSTRACT

Eleven new complexes of general formula $[Ag(NO_3)(L\text{-}Y)_2]$ corresponding to Ag(I) camphorimine complexes $[Ag(NO_3)(OC_{10}H_{14}NY)_2]$ (Y = $NMe_2$ (**1**); OH (**2**); $C_6H_5$ (**3**); 4-$MeC_6H_4$, (**4**); 3,5-$(CH_3)_2C_6H_3$ (**5**); 3-$OHC_6H_4$, (**6**); 3-$ClC_6H_4$ (**7**); 4-$ClC_6H_4$ (**8**); 4-$FC_6H_4$ (**9**); 4-$CF_3C_6H_4$ (**10**)) and the camphor sulfonylimine complex $[Ag(NO_3)(O_2SNC_{10}H_{14}NY)_2]$ (Y = $NH_2$) were synthesized/characterized and their structural properties and antibacterial activity studied to gain insights into the structure-antimicrobial activity relationships. Five of the complexes were selected as representative examples and structures were optimized by Density Functional Theory calculations. The results show that the imine substituents (Y) at the camphor ligands drive the structure of the complexes from distorted octahedral to trigonal prismatic or linear ionic while the effect of the sulfonylimine ring does not appreciably affects the geometry of the complex. The lipophilicity and polarity which are important parameters concerning the biological activity of the complexes are also high dependent of the characteristics of the camphor ligands. The redox properties of the complexes studied by cyclic voltammetry showed that their reduction potentials are essentially independent of their electronic and steric properties. The antibacterial activity of all the complexes, against Gram-positive (*S. aureus* Newman) and Gram-negative (*Escherichia coli* ATCC25922, *Pseudomonas aeruginosa* 477, *Burkholderia contaminans* IST408) strains was evaluated through calculation of MIC values. Results show that complexes with camphor imine ligands (**1** − **10**) that combine high lipophilicity with low dipolar moment (**3**–**5**) exhibit enhanced antibacterial activity. The ability to establish hydrogen bonding emerged as an important contribution to the antibacterial activity of the camphor sulphonylimine complex **11** (Y = $NH_2$).

## 1. Introduction

Complexes are chemical entities where metal and ligands bind to afford compounds with properties distinct from their precursors. Through the choice of the metal and the design of the ligands it is possible to drive the properties, reactivity and applications of the complexes. The characteristics of the metal are of utmost relevance concerning the biological interactions and toxicity of the complex.

Silver antiseptic properties are known since long ago. For instance, Hippocrates used silver in wound care, and the ancient Egyptians used silver vessels to preserve the quality of the drinking water. Due to its antimicrobial properties and general non-adverse effects for humans, silver and silver derivatives are presently used mainly as antimicrobials [1]. Examples of medical uses of silver compounds include coating of bandages to protect burns and wounds, coating of catheters as well as medical devices [1–3]. Non-medical uses may be found for example on coating of polyethylene fabrics for food packing [4]. A recent review reported that ca. fifty antimicrobial products based on silver were industrially patented [5].

Silver ions ($Ag^+$) are highly toxic to microorganisms, while the reduced form ($Ag^0$) is relatively inert [6]. The broad spectrum of antimicrobial activities of silver ions is due to the non-specific mechanisms that include the ability to bind to DNA, proteins and thiol groups, and generation of intracellular reactive oxygen species. These non-specific mechanisms interfere with enzymes and membrane proteins such as those involved in electron transport and energy generation and membrane ion exchange systems [7,8]. Recent studies highlighted that electron transfer processes [9] and interaction with efflux pumps [10] are important aspects in the antimicrobial activity of silver compounds. Yan and colleagues have recently reported the use of proteomics to investigate the cellular responses of *Pseudomonas aeruginosa* to silver nanoparticles. These authors found a total of 59 proteins as being regulated by silver, 5 of them involved in silver binding. Furthermore, the main pathways found as being involved in the antibacterial activity

* Corresponding authors.
*E-mail addresses:* fcarvalho@tecnico.ulisboa.pt (M.F.N.N. Carvalho), jorgeleitao@tecnico.ulisboa.pt (J.H. Leitão).

https://doi.org/10.1016/j.jinorgbio.2019.110791
Received 5 June 2019; Received in revised form 19 July 2019; Accepted 21 July 2019
Available online 22 July 2019

of silver nanoparticles were interference with the cell membrane functions, and the generation of intracellular reactive oxygen species [7]. In complexes, the characteristics of the ligands and the silver ions ($Ag^+$) combine, sometimes enhancing the antimicrobial activity of the complex compared to the silver precursors (e.g. $AgNO_3$), even when the free ligand is not active as in the case of camphor derivatives [11]. How the metal and the ligands cooperate to enhance the antimicrobial activity of the complexes remains unclear, although there is some consensus that the silver ion must be involved in the generation of reactive oxidative species, binding to DNA, interaction with cell membranes or the thiol groups of vital enzymes [1]. The ligands are thus thought to provide the complexes with characteristics suitable to act as carriers to deliver the silver ion into the cell. Therefore, complexes with weak binding ligands (nitrogen or oxygen) are expected to perform better than those with ligands that bind tightly to silver (phosphorus or sulphur). Such assumption is supported by a considerable number of Ag(I) complexes with N or O binding ligands reported as having antimicrobial properties [12]. Additionally, the formation of strong Ag—S bonds enabling the replacement of iron or zinc from proteins at the cell wall is one of the processes considered as responsible for silver antimicrobial activity [13].

Silver complexes with N-type ligands (camphor imines) fulfil the conditions to suitably deliver silver ions to the microbial cell. In fact, these complexes display relevant antimicrobial properties as corroborated by the high to moderate antibacterial or very high antifungal activities [14,15]. The characteristics of the camphor imine substituents (Y) in the delivery process of Ag(I) to the cells are still to understand. The results obtained till now point to distinct mechanisms underlying the antimicrobial activity of camphor imine silver complexes towards bacteria or fungi, since the complex with the highest antibacterial activity is distinct from that with the highest antifungal activity. We have also concluded that a geometry-activity relationship may exist, since complexes that differ just in the *meta* and *orto* position of the substituent at the aromatic ring in the camphor ligand, have considerably different antimicrobial activities. However, parameters such as hydrogen bridging, electron delocalization or the hydrophobic/hydrophilic character of the ligands are still to be evaluated. In the present work, new complexes were synthesized and their antibacterial activity was evaluated. The compounds were designed to get insights into the relationships between structural and electronic properties (hydrogen bridging, electron delocalization, and hydrophobicity/hydrophilicity) and antibacterial activity.

## 2. Results and discussion

### 2.1. Synthesis and characterization

A selection of camphor derivatives of the imine, hydrazone or sulphonyl imine types having distinct structural and electronic properties were used as ligands (Fig. 1) to prepare eleven new complexes that differ in the mono camphor character from those whose antimicrobial properties were studied before [11].

The structural characterization of the camphor imine ($OC_{10}H_{14}NY$) ligands Y = 4-$CH_3C_6H_4$ and Y = 3-$ClC_6H_4$ was made by X-rays diffraction analysis and their ORTEP drawings and relevant bond lengths and angles are depicted in Fig. 2 (cif file is available from CCDC).

The new complexes fit in the formula $[Ag(NO_3)(OC_{10}H_{14}NY)_2]$ (Y = $NMe_2$, **1**; OH, **2**; $C_6H_5$, **3**; 4-$MeC_6H_4$, **4**; 3,5-$(CH_3)_2C_6H_3$), **5**; 3-$OHC_6H_4$, **6**; 3-$ClC_6H_4$, **7**; 4-$ClC_6H_4$, **8**; 4-$FC_6H_4$, **9**; 4-$CF_3C_6H_4$, **10**) or $[Ag(NO_3)(O_2SNC_{10}H_{14}NNH_2)_2]$ (**11**) that essentially differ in the imine (**1–10**) or sulfonylimine (**11**) character of the camphor ligand (Fig. 2).

The choice of the substituents (Y) at position 3 of the camphor skeleton (see number labelling at Fig. 1) was directed towards the synthesis of complexes where hydrogen (**2**, **6**, **11**) or halide (**7–10**) could facilitate biological interactions due to the distinct electronic and/or geometric characteristics of the complexes. Complexes **2–10** are of the imine type (-C=N-R) while complexes **1** and **11** are of the hydrazone type (-C=N-$NR_2$) and complex **11** is of the sulphonylimine type (Fig. 1). Complex **12** was also synthesized for comparative purposes since its structural characterization by X-rays [10] was obtained before. A relevant parameter concerning the interaction of compounds with the cells is their lipophilic/hydrophilic character. Lipophilic compounds can diffuse through the cytoplasmic membrane while the hydrophilic compounds do not. The characteristics of the camphor substituent (Y) may prompt considerably different lipophilicities as predicted from log P = log [octanol]/[water] calculated using ACDC software, thus tune the activity of the complex.

The complexes were characterized by elemental analysis (EA) and spectroscopic techniques (FTIR, NMR). According to the elemental analysis all complexes fit in the 2:1 ligand to metal ratio. By FTIR the camphor imine complexes (**1–10**) display bands in the ranges typical stretching frequencies for C=O ($\nu_{CO}$, 1707–1754 $cm^{-1}$) and C=N ($\nu_{CN}$, 1577–1654 $cm^{-1}$). The camphor sulphonylimine complex (**11**) displays two IR bands in the region of C=N stretching with values that differ considerably (C=$NSO_2$, 1637 $cm^{-1}$; C=N-N, 1575 $cm^{-1}$) due to the distinct electronic properties of the sulphonylimine and the hydrazone groups. Additional IR bands (1379–1385 $cm^{-1}$) evidence the nitrate ($NO_3^-$) group. By $^{13}C$ NMR the carbon atom of the *keto* (position 2, Fig. 2) and the imine (position 3, Fig. 2) groups of the camphor ligands display chemical shifts in the narrow ranges of 204–207 ppm (**1–10**) and 173–175 ppm (**2–9**), respectively. The chemical shifts of the carbon atoms (*C*=N-N: 145.2 ppm, **1**; 155.0 ppm, **10**; 141.8 ppm, **11**) of the hydrazone type complexes are lower than those of the imine groups evidencing a higher shielding. The chemical shift of the sulphonylimine carbon atom (*C*=N-$SO_2$: 186.4, **11**) is between the hydrazone and keto groups suggesting intermediate electron densities. The analytical and spectroscopic characteristics of the camphor hydrazone complexes (**1** and **11**) fit well in the chalice-type structural arrangement found for

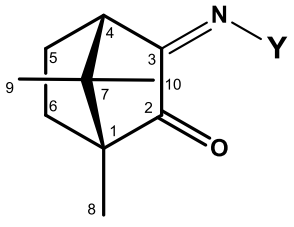


CAMPHOR IMINE Y= OH ($^2$L); $C_6H_5$ ($^3$L); 4-$MeC_6H_4$ ($^4$L); 3,5-$Me_2C_6H_3$ ($^5$L);3-$OHC_6H_4$ ($^6$L); 3-$ClC_6H_4$ ($^7$L); 4-$ClC_6H_4$ ($^8$L); 4-$FC_6H_4$ ($^9$L); 4-$CF_3C_6H_4$ ($^{10}$L);

CAMPHOR HYDRAZONE Y=$NMe_2$ ($^1$L)

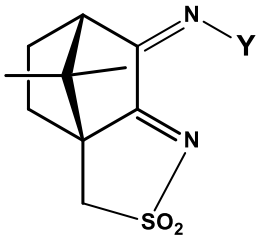


CAMPHOR SULPHONYLIMINE Y= $NH_2$ ($^{11}$L) or $NMe_2$ ($^{12}$L)

**Fig. 1.** Camphor imine (left) and camphor sulphonylimine (right) type-ligands used in this study.

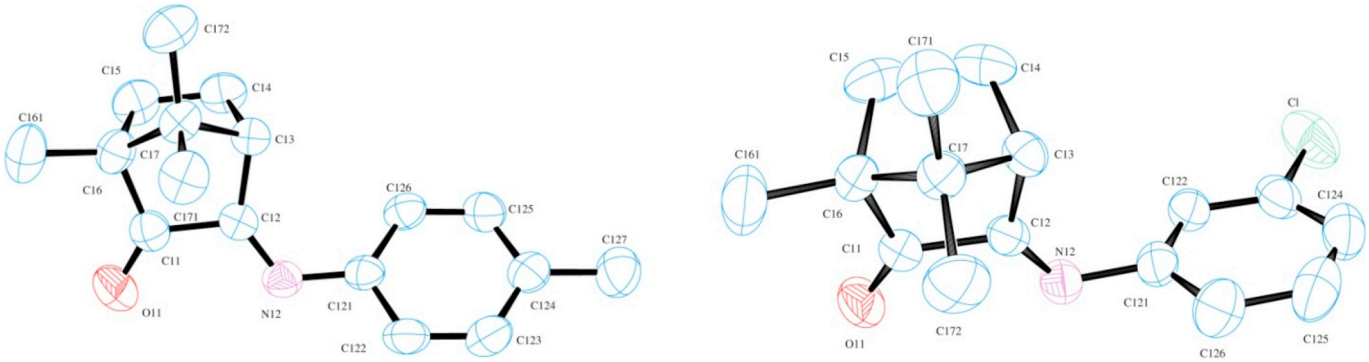


**Fig. 2.** ORTEP drawings (ellipsoids with 25% probability) for camphor ligands $OC_{10}H_{14}NY$: a) Y = 4-$CH_3C_6H_4$, [C═O, 120.5(3) pm; CN, 127.4(3) pm]; b) Y = 3-$ClC_6H_4$. [C═O, 119.7(39) pm; CN, 126.5(3) pm].

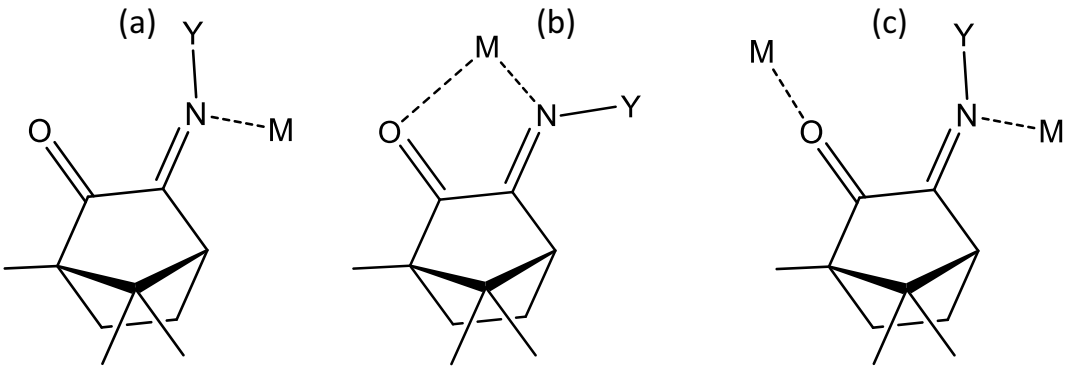


**Fig. 3.** Types of coordination of camphor imines: a)- mono-hapto; b)- di-hapto; c)- bridging.

$[Ag(NO_3)(O_2SNC_{10}H_{13}NNMe_2)_2]$ (**12**) [10].

The coordination of the camphor imine/hydrazone ligands to silver can involve the imine nitrogen atom as found for $[Ag(NO_3)(OC_{10}H_{13}NC_6H_4NC_{10}H_{13}O)]$ [16] (Fig. 3a), combined imine/keto as found for $[(CuCl)_2(Me_2NNC_{10}H_{14}O)]_n$ [17] or the *keto* group may enable coordination to the same (Fig. 3b) or sequential (Fig. 3c) silver atoms as found for metals of group 10 [18].

The characteristics of the imine substituent (Y), tunes the structural arrangement and may play a role in the interactions of the complex with the biological cell. Computational calculations were conducted to optimize the geometries of a selection of complexes in order to ascertain on the effect of different Y groups in the biological activity, if any.

### 2.2. Calculations

Compounds **1–4**, **8** and **12** were selected as representative of the different types of the Ag(I) camphor complexes under study and their geometries were optimized by DFT.

In the case of complexes with aromatic substituents (**3**, **4** and **8**) the aim was the study of the effect of the electron donor or donor characteristics of the substituent on the structural/antibacterial properties of the complexes.

The calculated and experimental data (obtained by X-ray diffraction analysis) [10] for complex $[Ag(NO_3)(O_2SNC_{10}H_{13}NNMe_2)_2]$ (**12**) are in good agreement (Table 1). The optimized relevant distances and angles for the selected complexes are displayed in Table 1.

According to the calculated bond lengths and angles, the geometry of the Ag(I) complexes vary from octahedral (**1**, **12**) to trigonal prismatic (**3**, **4**, **8**) or linear ionic (**2**). At complexes **1** and **12** (hydrazone type) the camphor ligands act as bidentate through the nitrogen of the imine and the oxygen atoms of the ketone groups (**1**) or through the nitrogen atoms of the imine and sulphonylimine groups (**12**) within a chalice-type arrangement (Fig. 2). The coordination sphere is completed by the $NO_3^-$ group that acts as a bidentate O—O ligand such as in the high distorted octahedral silver-nitrate complex $[Ag(NO_3)L_2]$ (L = 2-(bis(methylthio)methylene)-1-phenylbutane-1,3-dione [19]. Distortion from the octahedral geometry is lower in **1** (imine type) than in **12** (sulphonylimine type) (Fig. 4).

At complexes **3**, **4** and **8** of the camphor imine ligands that differ in the characteristics of the substituent (Y, aromatic) at the camphor skeleton, the ligands behave as mono dentate binding to silver through the imine nitrogen atoms with bond lengths that do not differ in the three complexes (Table 1). The oxygen atom of the camphor ketone group occupies a close non-binding distance such as in group 10 (Pd, Pt)

**Table 1**
Calculated distances/angles and dipole moment for complexes $[Ag(NO_3)(OC_{10}H_{14}NY)_2]$ (**1–4**, **8**) and $[Ag(NO_3)(O_2SNC_{10}H_{13}NNMe_2)_2]$ (**12**).

| Distance (Å)/ angles (°) | Y | | | | | |
|---|---|---|---|---|---|---|
| | $NMe_2$ (**1**) | OH (**2**) | $C_6H_5$ (**3**) | 4-$MeC_6H_5$ (**4**) | 4-$ClC_6H_5$ (**8**) | $NMe_2$ (**12**) |
| Ag-N(Y) | 2.39/ 2.47 | 2.23 | 2.28/ 2.33 | 2.28/2.34 | 2.28/ 2.34 | 2.83 |
| Ag-Z[a] | 2.59/ 2.66 | 2.75/ 2.85 | 2.84/ 2.92 | 2.84/2.89 | 2.84/ 2.91 | 2.32 (2.40)[b] |
| Ag-O1$_{(NO3)}$ | 2.40 | 2.70 | 2.41 | 2.42 | 2.42 | 2.45 |
| Ag-O2$_{(NO3)}$ | 2.67 | 2.74 | 2.69 | 2.69 | 2.68 | 2.45 |
| C=N | 131 | 129 | 129 | 129 | 129 | 129 |
| C=O | 126 | 125 | 125 | 125 | 125 | – |
| N-Ag-N | 144.8 | 160.3 | 144.4 | 143.8 | 144.6 | 136.1 (138.2) |
| *Z*-Ag-Z[a] | 82.3 | 77.8 | 68.2 | 70.1 | 68.4 | 91.8 |
| Z-Ag-O | 167.9/ 136.5 | 139.4/ 132.7 | 162.5/ 144.2 | 158.4/ 148.8 | 162.2/ 144.2 | 128.7/ 127.7 |
| Dipole (D) | 10.00 | 10.03 | 11.37 | 11.37 | 14.11 | 15.40 |

[a] Z = O or N.
[b] Experimental data obtained by X-rays diffraction analysis [11].

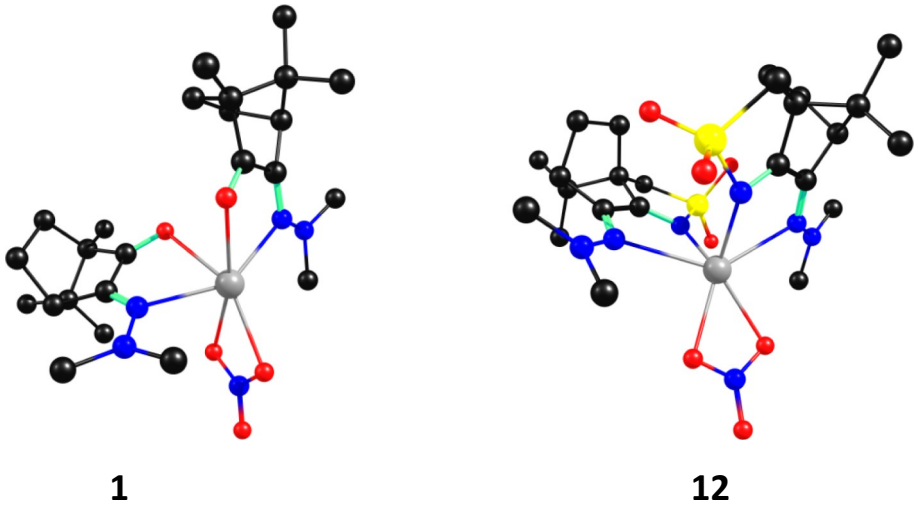


**Fig. 4.** Calculated structures for $[Ag(NO_3)(OC_{10}H_{13}NY)_2]$ (**1**) and $[Ag(NO_3)(O_2SNC_{10}H_{13}NY)_2]$ (**12**) (Y = $NMe_2$).

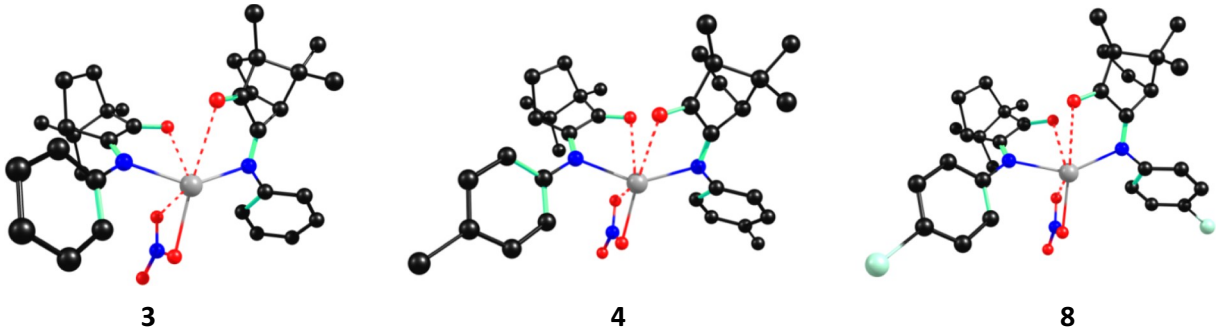


**Fig. 5.** Calculated structures for $[Ag(NO_3)(OC_{10}H_{13}NY)_2]$ (Y = $C_6H_5$, **3**; 4-$MeC_6H_4$, **4**; 4-$ClC_6H_4$, **8**).

complexes [20]. The geometries tend to trigonal prismatic (Fig. 5).

According to calculations, complex **2** (Y = OH) shows a considerably high cationic character (Q = 0.67). Therefore, the interaction of the nitrate group with the metal has an essentially outer sphere (non-bonding) character (Fig. 6).

Results from calculations clearly evidence that the characteristics of the camphor substituents (Y) drive the geometry and the coordination numbers (NC) of the complexes as well as the dipole moment (Table 1). The coordination number varies from six (octahedral) to three (trigonal prismatic) or two (linear) fostering a variable number of coordinative vacant positions and interactions with the microbial cell wall. The dipole moment drives the polarity of the complexes which is of utmost relevance to biological interactions.

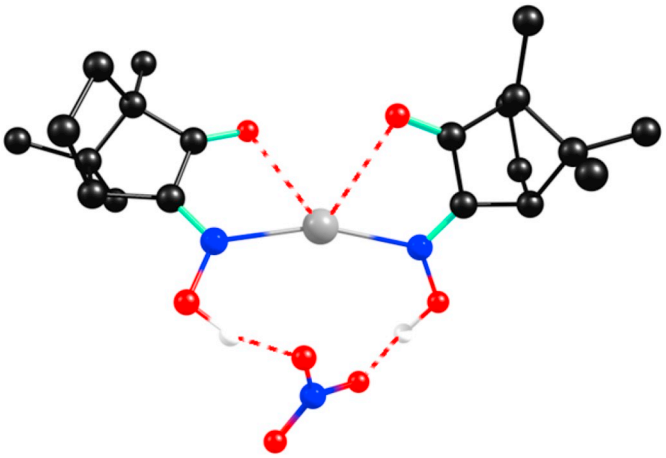

**Fig. 6.** Calculated structure for $[Ag(NO_3)(OC_{10}H_{13}NOH)_2]$ (**2**).

### 2.3. Structure - antibacterial activity relationships

Bacteria are commonly divided in Gram-positive and Gram-negative categories according to the characteristics of their cell wall. Both are composed of a cell membrane or cytoplasmitc membrane, which is surrounded by a thick layer of peptidoglycan and teichoic acids in the case of Gram-positive bacteria, while in the case of Gram-negative bacteria, a thin layer of peptidoglycan is contained in the periplasmic space that is surrounded by an outer membrane to which lipopolysaccharides are anchored. Gram-negative therefore have an additional barrier to antimicrobials which provides an extra protective layer keeping the vital role of material exchanges with the exterior of the cell. In order to gain insights into the relationships between structure of the silver camphor imine complexes and their antibacterial activity both Gram-negative and Gram positive bacteria were included in this study.

A relevant parameter concerning the interaction of compounds with the bacterial cell membrane is their lipophilic/hydrophilic character. Lipophilic compounds can cross the cytoplasmic membrane by diffusion while hydrophilic compounds need to be transported through the membrane to reach intracellular targets. At complexes, the substituent (Y) at the camphor imine ligand (Fig. 1) may prompt considerably different lipophilicities, as predicted from log P = log [octanol]/[water] (using ACDC software), thus tuning the antibacterial activity of the complex.

The antibacterial properties of the complexes $[Ag(NO_3)$

**Table 2**
Data for complexes $[Ag(NO_3)(OC_{10}H_{14}NY)_2]$.

| LIGAND Y | | $E_p^{red}$ Volt[a] | MIC (μg/mL) *E. coli ATCC25922* | *P. aeruginosa 477* | *B. contaminans IST408* | *S. aureus Newman* | Log P[b] |
|---|---|---|---|---|---|---|---|
| **1** | $NMe_2$ | | 58 | 54 | 41 | 134 | 0.97 ± 0.60 |
| **2** | OH | 0.11 | 51 | 52 | 59 | 119 | 1.06 ± 0.59 |
| **3** | $C_6H_5$ | 0.12 | 59 | 55 | 91 | 54 | 2.94 ± 0.58 |
| **4** | 4-$MeC_6H_4$ | | 37 | 53 | 66 | 55 | 3.40 ± 0.58 |
| **5** | 3,5-$Me_2C_6H_3$ | 0.11 | 40 | 52 | 105 | 47 | 3.86 ± 0.59 |
| **6** | 3-$OHC_6H_4$ | 0.074 | 52 | 53 | 75 | 113 | 2.36 ± 0.59 |
| **7** | 3-$ClC_6H_4$ | 0.044 | 53 | 53 | 44 | 110 | 3.65 ± 0.59 |
| **8** | 4-$ClC_6H_4$ | 0.12 | 52 | 55 | 57 | 151 | 3.78 ± 0.59 |
| **9** | 4-$FC_6H_4$ | 0.097 | 59 | 53 | 77 | 93 | 3.24 ± 0.62 |
| **10** | 4-$CF_3C_6H_4$ | 0.11 | 52 | 60 | 55 | 105 | 3.91 ± 0.61 |

[a] Potential in Volt ( ± 10 mV) vs sce.
[b] Partition coefficient in octanol/water predicted using ACDC software.

**Table 3**
Data for complexes $[Ag(NO_3)(O_2SNC_{10}H_{13}NY)_2]$.

| LIGAND Y | | $E_p^{red}$ Volt[a] | MIC (μg/mL) *E. coli ATCC25922* | *P. aeruginosa 477* | *B. contaminans IST408* | *S. aureus Newman* | Log P[b] |
|---|---|---|---|---|---|---|---|
| **11** | $NH_2$ | 0.10 | 52 | 36 | 38 | 114 | −0.99 ± 0.69 |
| **12** | $NMe_2$ | 0.17 | 107 | 108 | 56 | 257 | −0.69 ± 0.70 |
| | $[Ag(NO_3)]$ | 0.18 | 47 | 39 | 74 | 73 | – |

[a] Potential in Volt ( ± 10 mV) vs sce.
[b] Predicted partition coefficient in octanol/water using ACDC software.

$(OC_{10}H_{14}NY)_2]$ (**1–10**) and $[Ag(NO_3)(O_2SNC_{10}H_{13}NY)_2]$ (**11,12**) towards the Gram-positive *Staphylococcus aureus* Newman, and the Gram-negative *Pseudomonas aeruginosa* 477, *Escherichia coli* ATCC25922, and *Burkholderia contaminans* IST408, were assessed by determining the MIC values by microplate dilution assay and by fitting the data with a modified Gompertz equation as previously described [14]. All complexes display antibacterial activities (Tables 2 and 3).

A first insight into Table 2 shows that the antimicrobial activity of the complexes (**1–10**) towards *P. aeruginosa* is almost independent of the characteristics of the camphor ligands and the structure of the complexes, in contrast to the other bacterial strains. Such behaviour points to the mechanisms underlying the antimicrobial activity of the complexes towards *P. aeruginosa* as being essentially distinct from those towards *E. coli*, *S. aureus* or *B. contaminans* (Tables 2). A *Pseudomonas*-specific process apparently overwhelms other mechanisms involved in the antimicrobial activity of the silver camphorimine complexes and drives a structure-independent process while for the other strains the characteristics of the complexes modulated their antibacterial activity. A trait specific of *P. aeruginosa* strains is their ability to secrete pyocyanin, a redox active compound involved in the activation of molecular oxygen and formation of hydrogen peroxide. A recent study by Muller [5] showed that the silver ion ($Ag^+$) competes with molecular oxygen by electron transfer from pyocyanin and concomitantly decreases the production of hydrogen peroxide from molecular oxygen. A redox process mediated by pyocyanin leading to $Ag^+ \rightarrow Ag^0$ reduction, decomposition of the camphorimine complex and generation of a naked silver species (conceivably of the nano size) can explain the complexes-independent anti-*P. aeruginosa* activity. To support such proposal the redox properties of a selection of the complexes were studied by cyclic voltammetry. The results show that the potentials at which the silver metal sites reduce (Tables 2 and 3) are slightly higher than the potential at which pyocyanin oxidizes (E = −0.34 V) [5] thus accounting for a favourable redox process between them. Such process conceivably buffers the activity of the complexes due to less $Ag^+$ ion being available to promote electron capture and cell wall impairment which is one of the mechanisms responsible for the antimicrobial action of silver compounds [21]. That is not the case of the camphor sulphonylimine complexes **11** and **12** that reveal structural dependent activity towards *P. aeruginosa*. Complex **11** exhibits MIC values almost 3 times lower than complex **12** (36 and 108 μg/mL, respectively, Table 3). The main structural difference between **11** and **12** refers to the Y group at the amine substituent (Fig. 1) that at complex **11** (Y = $NH_2$) is prone to establish hydrogen bonding with carboxyl or amino groups of proteins or other molecular components of the bacterial cells enabling the antibacterial activity of the complex against *P. aeruginosa*. Non-covalent bonding is less feasible in the case of **12** (Y = $NMe_2$) thus the antibacterial activity is much lower. Further support to hydrogen bonding relevance towards the antibacterial activity of the complexes is obtained from the MIC values of complexes **11** and **12** (Table 3) where **11** performs better than complex **12** for the Gram-positive and Gram-negative strains studied. From the set of complexes under study, complexes **2** (Y = OH) and **6** ($C_6H_4OH$) could in principle establish hydrogen bridges with the cell components. However, the cationic character/linear geometry of **2** and the low acidity of **6** (due to electron delocalization through the aromatic ring) decrease hydrogen bonding establishment.

Complexes **3–5** display the lowest MIC values towards the Gram-positive *S. aureus* which are ca. half of the values calculated for complexes **6–10** (Table 2). Since, the geometry of complexes **3–10** is trigonal prismatic according to calculations (Fig. 5) their distinct activities must rely on the characteristics of the aromatic imine group (Fig. 1) that is essentially non-polar [$C_6H_4R$: *R* = 4-H (**3**), R = 4-Me (**4**), *R* = 3,5-$Me_2$ (**5**)] or polar [R = 3-OH (**6**), R = 3-Cl (**7**), R = 4-Cl (**8**), R = 4-F (**9**), R = 4-$CF_3$ (**10**)].

Complexes **1–10** perform better towards *Gram-negative* than *Gram-positive* bacteria, except complexes **3–5** that display similar activities towards *S. aureus*, *E. coli* and *P. aeruginosa* (Table 2). In fact, complexes **4** and **5** display the lowest MIC values towards Gram-negative *E. coli* (37 and 40 μg/mL, respectively) and additionally **5** displays the lowest value against *S. aureus* (47 μg/mL). These data points to high

lipophilicity (estimated [15] through calculation of logP values, Tables 2 and 3) associated with low polarity as structural features favouring the antibacterial activity of the silver complexes. High lipophilicity enables molecules to cross the membrane by diffusion to reach the bacterial cytoplasm [22] while hydrophilic compounds such as β-lactams need to use the outer membrane porins or other transport systems to gain access to the interior of the bacterial cell.

The activity of the silver camphor imine complexes (**1 − 12**) towards *B. contaminans* contrasts with the above mentioned, since low lipophilicity irrespectively of the polarity, tends to favours the antimicrobial activity of the complexes (**1**, **2**, **11**, **12**) with hydrogen bridging also playing a role in the process, as observed for complex **11** that displays the lowest MIC values towards *B. contaminans* (Table 3). This strain belongs to a large group of species known as the *Burkholderia cepacia* complex, characterized by possessing large genomes encoding more than 7500 genes and encompassing numerous membrane transport systems which might be "highjacked" by hydrophilic camphor complexes [23].

The results presented herein show that bacterial resistance to antimicrobials is multifactorial and often strain-specific including intrinsic resistance as a result of structural features such as poor membrane permeability, constitutive expression of efflux pumps, high resistance due to the acquisition of resistance genes or genetic modifications and active efflux mechanisms [24].

The antimicrobial activities of complexes **1–12** reflect the differences in the mechanisms used by each strain to resist to the antimicrobials and additionally show that the relationships between the structures of the complexes and their activity are highly dependent of the strain. Therefore, generalization is not possible since a wide variety of mechanisms can be used by each bacterial stain, the compounds they secret, electron transfer processes between the cell and the complexes and many other parameters. However, it is evident from the herein results that the activity of the Ag(I) camphor imine can be tuned towards Gram-positive or Gram-negative bacteria through design of the camphor ligands.

## 3. Conclusions

Two sets of new silver camphor complexes $[Ag(NO_3)(L\text{-}Y)_2]$, that essentially differ on the ligands [camphor imine ($OC_{10}H_{14}NY$); camphor sulphonylimine ($SO_2NC_{10}H_{14}NY$)] were designed, synthesized/characterized and their antibacterial properties evaluated through calculation of the MIC values. All complexes display antimicrobial activity towards Gram-positive (*Staphylococcus aureus Newman*) and Gram-negative bacteria (*Pseudomonas aeruginosa* 477, *Escherichia coli* ATCC 25922, *Burkholderia contaminans* IST408) with magnitudes that vary according to the characteristics of the substituent (Y) of the camphor imine ligand and the bacteria strain.

The structures of a selection of complexes (**1–4**, **8** and **12**) were optimized by Density Functional Theory. Data revealed that the geometries considerably vary according to the substituent (Y) at the imine group (NY). Hydrazone type substituents ($Y = NR_2$) prompt complexes with octahedral distorted geometries (**1**, **12**) and coordination number equal to six due to cooperative binding of the nitrogen and oxygen atoms of the imine ligand (**1**) or the two nitrogen atoms of the sulphonylimine ligand (**12**), while nitrate ($NO_3^-$) binds through two oxygen atoms. Complex **2** (Y = OH) has a cationic character with a linear geometry, the ligand binding the silver atom through the imine nitrogen atom, the $NO_3^-$ ion occupying the outer sphere of the complex. Complexes **3**, **4** and **8** display trigonal prismatic geometries ($Y = C_6H_4R$) with the ligands (L) binding the metal through the nitrogen atom and the nitrate through one of the oxygen atoms.

As a general trend, the Ag(I) complexes (**1–12**) perform better towards Gram-negative than Gram-positive bacteria. Exceptions are complexes **3–5** that display similar MIC values for *P. aeruginosa*, *E. coli* and *S. aureus*. The combined high lipophilicity and low polarity of complexes **3–5** is considered to enhance their activity towards *S. aureus*. These parameters also seem relevant for the lowest MIC values displayed by complexes **4** and **5** against *E. coli*. Hydrogen bonding in **11** is considered to account for the enhanced activity against *P. aeruginosa* (MIC, 36 μg/mL) and *B. contaminans* (MIC, 38 μg/mL) compared to the related complex **12**.

In contrast to the sensitivity of the geometry and the antibacterial activity of the complexes to the electronic and steric characteristics of the imine substituents (Y), Y-independent antibacterial activity of complexes **1–10** was found towards *P. aeruginosa*. Such behaviour was attributed to reduction of the silver site by the redox active pyocyanin secreted by *P. aeruginosa*. Such electron transfer process is feasible according to the redox potentials of the complexes measured by cyclic voltammetry.

In what concerns the geometry and the antimicrobial activity of the complexes no direct relationship was found, however, there is a relationship between the characteristics of the camphor imine substituents (Y) the geometry and the antibacterial activity of the complexes (**1–10**). Complexes with camphor imine ligands combining high lipophilicity with low dipolar moment (**3–5**) exhibit low MIC values, thus high activity towards Gram-positive *S. aureus*, while camphor imine complexes with high polarity (**6–10**) perform better towards Gram-negative bacteria. The high polarity and low lipophilicity of the camphor sulphonylimine complexes (**11**, **12**) apparently favour the activity against Gram-negative bacteria with further enhancement due hydrogen bonding in the case of complex **11**. Therefore, the rational design of complexes driving their activity towards Gam-positive or Gram-negative is feasible through choice of the suitable substituent (Y) of the camphor imine or camphor sulphonylimine ligand.

## 4. Experimental

The complexes were synthesized under nitrogen using Schlenk and vacuum techniques. Camphor ligands ($OC_{10}H_{14}NY$: Y═OH, $C_6H_5$, $NH_2$, $NMe_2$ and $O_2SNC_{10}H_{14}NNH_2$) were prepared according to reported procedures [20, 25]. Silver nitrate, (1*R*)-(+)-camphor, (1*S*)-(+)-10-sulfonic acid and amines were purchased from Sigma Aldrich. Acetonitrile (PA grade) was purchased from Carlo Erba purified by conventional techniques [26] and distilled before use. The FTIR spectra were obtained from KBr pellets using a JASCO FT/IR 4100 spectrometer. The NMR spectra ($^1H$, $^{13}C$, $^{19}F$, DEPT, HSQC and HMBC) were obtained from $CD_2Cl_2$, $CD_3CN$, Acetone-$d_6$ or $CDCl_3$ solutions using a Bruker Avance II+ (300 or 400 MHz) spectrometers. NMR chemical shifts are referred to TMS (δ = 0 ppm). The redox properties were studied by cyclic voltammetry using a three compartments cell equipped with a Pt wire electrode and interfaced with a VoltaLab PST050 equipment. The cyclic voltammograms were obtained using $NBu_4BF_4$ as electrolyte (0.10 M) in $CH_3CN$. The potentials were measured in Volts (± 10 mV) versus SCE at 200 mV/s using $(Fe(\eta^5\text{-}C_5H_5)_2]^{0/+}$ ($E_{1/2}{}^{red}$ = 0.382 V; $CH_3CN$) as internal reference.

### 4.1. Synthesis

#### 4.1.1. Camphor derivatives

The new camphor imines were obtained from camphorquinone by reaction with the appropriate amine or hydrazine in ethanol, using Forster procedures [27] and improvements [11,28,29].

Characterization details:

**$OC_{10}H_{14}NC_6H_4CH_3$-4**

Elem. Anal. (%) for $C_{17}H_{21}NO$: Found.: C, 80.4; N, 5.5H, 8.3. Calc.: C, 80.0; N, 5.5; H, 8.2.IR ($cm^{-1}$): 1748 (C=O), 1652 (C=N). $^1H$ NMR ($CDCl_3$, $\delta_{ppm}$): 7.15 (d, *J* = 8.0 Hz, 2H); 6.84 (d, *J* = 8.0 Hz, 2H); 2.84 (d, *J* = 4.7 Hz, 1H); 2.33 (s, 3H); 2.17–2.01 (m, 1H); 1.91–1.77 (m, 1H); 1.72–1.55 (m, 2H) 1.08 (s, 3H); 0.96 (s, 3H); 0.87 (s, 3H). $^{13}C$ NMR ($CDCl_3$, $\delta_{ppm}$): 206.3 (C=O); 171.4 (C=N); 146.6, 135.4 ($CPh_{ipso}$); 129.6, 120.9 (CPh); 58.0 (C1); 50.2 (C4); 44.8 (C7); 30.2 (C6); 24.4

(C5); 21.0, 17.6 (C9, C10); 9.1 (C8).

**$OC_{10}H_{14}NC_6H_3(CH_3)_2$ -3,5**

Elem. Anal. (%) for $C_{18}H_{23}ON$: Found.: C, 80.3; N, 5.5; H, 9.0. Calc.: C, 80.3; N, 5.2; H, 8.6; IR ($cm^{-1}$): 1748 (C=O); 1663 (C=N); 1601 (Ph); $^1H$ NMR ($CDCl_3$, $\delta_{ppm}$): 6.79 (s, 1H); 6.50 (s, 2H); 2.80 (d, $J$ = 4.7 Hz, 1H); 2.29 (s, 6H); 2.10–2.01 (m, 1H); 1.88–1.78 (m, 1H); 1.68–1.56 (m, 2H); 1.08 (s, 3H); 0.96 (s, 3H); 0.88 (s, 3H); $^{13}C$ NMR ($CDCl_3$, $\delta_{ppm}$): 206.6 (C=O); 171.4 (C=N); 149.6, 138.6 ($CPh_{ipso}$); 126.9, 117.9 (CPh); 58.1 (C1); 50.1 (C4); 44.5 (C7); 30.1, 24.4 (C5, C6); 21.4 ($(CH_3)_2$); 21.0, 17.5 (C9, C10); 9.1 (C8).

**$OC_{10}H_{14}NC_6H_4OH$-3**

Elem. Anal. (%) for $C_{16}H_{19}O_2N{\cdot}1/5H_2O$: Found.: C, 73.6; N, 5.7; H, 7.6. Calc.: C, 73.7; N, 5.4; H, 7.4. IR ($cm^{-1}$): 3361 (OH); 1748 (C=O); 1666 (C=N); 1580 (Ph). $^1H$ NMR ($CDCl_3$, $\delta_{ppm}$): 7.17 (t, $J$ = 8.0 Hz, 1H); 6.64 (d, $J$ = 8.0 Hz, 1H); 6.47–6.38 (m, 2H); 2.82 (d, $J$ = 4.7 Hz, 1H); 2.11–2.01 (m, 1H); 1.88–1.77 (m, 1H); 1.68–1.53 (m, 2H); 1.07 (s, 3H); 0.96 (s, 3H); 0.87 (s, 3H). $^{13}C$ NMR ($CDCl_3$, $\delta_{ppm}$): 206.5 (C=O); 172.2 (C=N); 156.5, 150.7 ($CPh_{ipso}$); 130.0, 112.6, 112.3, 107.8 (CPh); 58.2 (C1); 50.2 (C4); 44.5 (C7); 30.1, 24.4 (C5, C6); 21.0, 17.5 (C9, C10); 9.0 (C8).

**$OC_{10}H_{14}NC_6H_4CF_3$-4**

Elem. Anal. (%) for $C_{17}H_{18}F_3ON{\cdot}¼H_2O$: Found.: C, 64.8; N, 4.6; H, 5.5. Calc.: C, 65.1; N, 4.5; H, 5.9; IR ($cm^{-1}$): 1752 (C=O); 1672 (C=N); 1609 (Ph); 1325, 1112 ($CF_3$); $^1H$ NMR ($CDCl_3$, $\delta_{ppm}$): 7.60 (d, $J$ = 8.3 Hz, 2H); 6.94 (d, $J$ = 8.3 Hz, 2H); 2.70 (d, $J$ = 4.6 Hz, 1H); 2.13–2.02 (m, 1H); 1.93–1.80 (m, 1H); 1.73–1.51 (m, 2H); 1.10 (s, 3H); 0.97 (s, 3H); 0.91 (s, 3H); $^{13}C$ NMR ($CDCl_3$, $\delta_{ppm}$): 205.8 (C=O); 173.2 (C=N); 152.9, 126.9 ($CPh_{ipso}$); 126.3 (q, $J$ = 3.8 Hz) ($CF_3$); 120.0 (CPh); 58.2 (C1); 50.1 (C4); 44.5 (C7); 30.0, 24.4 (C5, C6); 21.1, 17.4 (C9, C10); 9.0 (C8).

**$OC_{10}H_{14}NC_6H_4F$-4**

Elem. Anal. (%) for $C_{16}H_{18}ONF{\cdot}½H_2O$: Found.: C, 71.4; N, 5.7; H, 7.0. Calc.: C, 71.6; N, 5.2; H, 7.1; IR ($cm^{-1}$): 1747 (C=O); 1655 (C=N); 1591 (Ph); $^1H$ NMR ($CDCl_3$, $\delta_{ppm}$): 7.05 (t, $J$ = 8.3 Hz, 2H); 6.94–6.89 (m, 2H); 2.82 (d, $J$ = 4.6 Hz, 1H); 2.15–2.06 (m, 1H); 1.91–1.82 (m, 1H); 1.71–1.56 (m, 2H); 1.09 (s, 3H); 0.98 (s, 3H); 0.88 (s, 3H); $^{13}C$ NMR ($CDCl_3$, $\delta_{ppm}$): 206.2 (C=O); 172.1 (C=N); 145.3, 126.2 ($CPh_{ipso}$); 122.5, 122.4, 115.9, 115.7 (CPh); 58.0 (C1); 50.1 (C4); 44.7 (C7); 30.2, 24.3 (C5, C6); 21.0, 17.5 (C9, C10); 9.1 (C8).

**$OC_{10}H_{14}NC_6H_4Cl$-4**

Elem. Anal. (%) for $C_{16}H_{18}ONCl$: Found: C, 69.5; 5.0; 6.5; Calc.: C, 69.7; N, 5.1; H, 6.5; IR ($cm^{-1}$): 1747 (C=O); 1673 (C=N); 1662 (C=N); $^1H$ NMR (Acetone-$d_6$, $\delta_{ppm}$): 7.41 (d, $J$ = 8.6 Hz, 2H); 6.91 (d, $J$ = 8.6 Hz, 2H); 2.82 (sbr, 1H); 2.17–2.09 (m, 1H); 1.96–1.88 (m, 1H); 1.68–1.54 (m, 2H); 1.03 (s, 3H); 1.01 (s, 3H); 0.87 (s, 3H); $^{13}C$ NMR (Acetone-$d_6$, $\delta_{ppm}$): 205.8 (C=O); 173.6 (C=N); 150.0, 130.7 ($CPh_{ipso}$); 130.0, 122.6 (CPh); 58.6 (C1); 51.0 (C4); 45.0 (C7); 30.7, 24.7 (C5, C6); 21.0, 17.6 (C9, C10); 9.3 (C8).

**$OC_{10}H_{14}NC_6H_4Cl$-3**

Elem. Anal. (%) for $C_{16}H_{18}ONCl{\cdot}1/20\ CHCl_3$: Found.: C, 68.7; N, 5.1; H, 6.6. Calc.: C, 68.4; N, 5.0; H, 6.4. IR ($cm^{-1}$): 1754 (C=O); 1681 (C=N); 1589 (Ph); $^1H$ NMR ($CDCl_3$, $\delta_{ppm}$): 7.20 (t, $J$ = 8 Hz, 1H); 7.13 (d, $J$ = 8 Hz, 1H); 6.88 (d, $J$ = 1.8 Hz, 1H); 6.76 (d, $J$ = 7.6 Hz, 1H); 2.77 (d, $J$ = 4.8 Hz, 1H); 2.14–2.03 (m, 1H); 1.91–1.81 (m, 1H); 1.70–1.53 (m, 2H); 1.09 (s, 3H); 0.98 (s, 3H); 0.90 (s, 3H); $^{13}C$ NMR ($CDCl_3$, $\delta_{ppm}$): 206.0 (C=O); 172.9 (C=N); 151.0, 134.7 ($CPh_{ipso}$); 130.1, 125.2, 120.3, 118.4 (CPh); 58.2 (C1); 50.1 (C4); 44.5 (C7); 30.1, 24.4 (C5, C6); 21.0, 17.5 (C9, C10); 9.0 (C8).

*4.1.2. Complexes*

The complexes were synthesized using the following typical procedure: $AgNO_3$ (0.50 mol) was added to the solution of the suitable ligand (1.0 mol) in acetonitrile (ca. 5 ml). Then the mixture was protected from light, stirred for ca. 2 h at RT and filtered (if necessary) to remove silver particles. The solvent was then evaporated till precipitation starts. Cooling in the fridge for ca. 1 day favours precipitation of the yellowish complexes that may then be obtained by filtration (Yield =50–65%). Characterization details:

**$[Ag(NO_3)(OC_{10}H_{14}NNMe_2)_2]$ (1)**

Elem. Anal. (%) for $AgC_{20}H_{40}N_5O_5 \cdot 2H_2O$: Found.: C, 46.1; N, 11.1; H, 6.6; Calc.: C, 46.3; N, 11.3; H, 7.1; IR ($cm^{-1}$): 1707 (C=O); 1566 (C=N); 1385 ($NO_3$); $^1H$ NMR ($CD_3CN$, $\delta_{ppm}$): 3.22 (d, $J$ = 4.3, 1H); 3.12 (s, 6H); 2.14–2.02 (m, 1H); 1.83–1.71 (m, 1H); 1.56–1.46 (m, 1H); 1.42–1.31 (m, 1H); 0.95 (s, 3H); 0.94 (s, 3H); 0.81 (s, 3H); $^{13}C$ NMR ($CD_3CN$, $\delta_{ppm}$): 206.3 (C=O); 145.2 (C=N); 57.5 (C1); 51.7 (C4); 46.9 ($(CH_3)_2$); 46.7 (C7); 30.8 (C6); 26.4 (C5); 21.0, 18.1 (C9, C10); 9.6 (C8).

**$[Ag(NO_3)(OC_{10}H_{14}NOH)_2]$ (2)**

Elem. Anal. (%) for $AgC_{20}H_{30}N_3O_7$: Found.: C, 45.1; N, 7.3; H, 5.7; Calc.: C, 45.1; N, 7.9; H, 5.6. IR ($cm^{-1}$): 3433 (OH); 1743 (C=O); 1643(C=N); 1379 ($NO_3$); $^1H$ NMR ($CD_3CN$, $\delta_{ppm}$): 10.33 (s, 1H); 3.19 (d, $J$ = 4.3 Hz, 1H); 2.22 (s, 1H); 2.14–1.73 (3); 1.50–1.37 (1); 0.99 (s, 3H); 0.96 (s, 3H); 0.82 (s, 3H); $^{13}C$ NMR ($CD_3CN$, $\delta_{ppm}$): 205.3 (C=O); 160.6 (C=N); 59.2 (C1); 47.5 (C4); 45.5 (C7); 31.4 (C6); 24.4 (C5); 20.8, 17.7 (C9, C10); 9.3 (C8).

**$[Ag(NO_3)(OC_{10}H_{14}NC_6H_5)_2]$ (3)**

Elem. Anal. (%) for $AgC_{32}H_{38}N_3O_5$: Found.: C, 58.7; N, 6.7; H, 6.1. Calc.: C, 58.9; N, 6.4; H, 5.8; IR ($cm^{-1}$): 1746 (C=O); 1659 (C=N); 1592 (Ph); 1379 ($NO_3$). $^1H$ NMR ($CD_2Cl_2$, $\delta_{ppm}$): 7.38 (d, $J$ = 7.8 Hz, 2H); 7.25 (t, $J$ = 7.3 Hz, 1H); 7.03 (d, $J$ = 8 Hz, 2H); 2.885 (d, $J$ = 4.8 Hz, 1H); 2.17–2.07 (m, 1H); 1.95–1.85 (m, 1H); 1.69–1.53 (m, 2H); 1.07 (s, 3H); 0.97 (s, 3H); 0.82 (s, 3H); $^{13}C$ NMR ($CD_2Cl_2$, $\delta_{ppm}$): 205.6 (C=O); 174.4 (C=N); 148.1 ($CPh_{ipso}$); 129.7, 127.3, 121.9 (CPh); 58.5 (C1); 51.2 (C4); 45.2 (C7); 30.5 (C6); 24.6 (C5); 21.4, 17.4 (C9, C10); 9.1 (C8).

**$[Ag(NO_3)(OC_{10}H_{14}NC_6H_4CH_3$-4$)_2]$ (4)**

Elem. Anal. (%) for $AgC_{34}H_{42}N_3O_5{\cdot}⅓HNO_3$: Found.: C, 58.5; N, 7.1; H, 6.4. Calc.: C, 58.2; N, 6.7; H, 6.0. IR ($cm^{-1}$): 1747 (C=O); 1654 (C=N); 1384 ($NO_3$). $^1H$ NMR ($CD_2Cl_2$, $\delta_{ppm}$): 7.17 (d, $J$ = 8.0 Hz, 2H); 6.96 (d, $J$ = 8.0 Hz, 2H); 2.91 (d, $J$ = 4.8 Hz, 1H); 2.33 (s, 3H); 2.21–2.05 (m, 1H); 1.93–1.80 (m, 1H); 1.65–1.50 (m, 2H); 1.05 (s, 3H); 0.97 (s, 3H); 0.78 (s, 3H). $^{13}C$ NMR ($CD_2Cl_2$, $\delta_{ppm}$): 205.5 (C=O); 173.3 (C=N); 145.2, 137.8 ($CPh_{ipso}$); 130.2, 122.4 (CPh); 58.4 (C1); 51.3 (C4); 45.3 (C7); 30.5 (C6); 24.4 (C5); 21.3, 21.1, 17.4 ($CH_3$, C9, C10); 9.0 (C8).

**$[Ag(NO_3)(OC_{10}H_{14}NC_6H_3(CH_3)_2$-3,5$)_2]$ (5)**

Elem. Anal. (%) for $AgC_{36}H_{46}N_3O_5\ 2H_2O$: Found.: C, 57.9; N, 5.9; H, 6.4; Calc.: C, 58.1; N, 5.6; H, 6.7; IR ($cm^{-1}$): 1754 (C=O); 1680 (C=N); 1592 (Ph); 1383 ($NO_3$); $^1H$ NMR ($CD_3CN$, $\delta_{ppm}$): 6.88 (s, 1H); 6.54 (s, 2H); 2.80 (d, $J$ = 4.4 Hz, 1H); 2.30 (s, 6H); 2.12–2.04 (m, 1H); 1.92–1.86 (m, 1H); 1.63–1.54 (m, 2H); 1.05 (s, 3H); 0.98 (s, 3H); 0.84 (s, 3H); $^{13}C$ NMR ($CD_3CN$, $\delta_{ppm}$): 207.3 (C=O); 173.4 (C=N); 150.3, 140.0 ($CPh_{ipso}$); 128.0, 118.9 (CPh); 58.9 (C1); 51.2 (C4); 45.2 (C7); 30.8 (C6); 24.8 (C5); 21.3 ($(CH_3)_2$); 21.2, 17.4 (C9, C10); 9.3 (C8).

**$[Ag(NO_3)(OC_{10}H_{14}NC_6H_4OH$-3$)_2]$ (6)**

Elem. Anal. (%) for $AgC_{32}H_{38}N_3O_7 \cdot 3/2H_2O$: Exp.: C, 53.8; N, 5.9; H, 4.9. Calc.: C, 54.0; N, 5.9; H, 4.6. IR ($cm^{-1}$): 3375 (OH); 1750 (C=O); 1664 (C=N); 1588 (Ph); 1384 ($NO_3$). $^1H$ NMR ($CD_2Cl_2$, $\delta_{ppm}$): 7.22 (t, $J$ = 7.8 Hz, 1H); 6.89 (s, 1H) 6.81 (s, 1H); 6.47 (d, $J$ = 7.3 Hz, 1H); 3.01 (d, $J$ = 4.6 Hz, 1H); 2.25–2.14(m, 1H); 1.99–1.88 (m, 1H); 1.71–1.58 (m, 2H); 1.07 (s, 3H); 1.01 (s, 3H); 0.78 (s, 3H); $^{13}C$ NMR ($CD_2Cl_2$, $\delta_{ppm}$): 205.6 (C=O); 174.4 (C=N); 158.8, 148.5 ($CPh_{ipso}$); 130.5, 115.5, 112.5, 109.9 (CPh); 58.5 (C1); 51.6 (C4); 45.3 (C7); 30.6 (C6); 24.4 (C5); 21.3, 17.2 (C9, C10); 9.0 (C8).

**$[Ag(NO_3)(OC_{10}H_{14}NC_6H_4Cl$-3$)_2]$ (7)**

Elem. Anal. (%) for $AgC_{32}H_{36}N_3O_5Cl_2 \cdot 2H_2O$: Found.: C, 50.7; N, 5.8; H, 5.1; Calc.: C, 50.7; N, 5.5; H, 5.3; IR ($cm^{-1}$): 1755 (C=O); 1684 (C=N); 1590 (Ph); 1381 ($NO_3$); $^1H$ NMR ($CD_3CN$, $\delta_{ppm}$): 7.38 (t, $J$ = 8.0 Hz, 1H); 7.22 (d, $J$ = 8.0 Hz, 1H); 6.95 (s, 1H); 6.83 (d, $J$ = 7.9, 1H); 2.75 (d, $J$ = 4.7 Hz, 1H); 2.09–2.03 (m, 1H); 1.92–1.87 (m, 1H); 1.65–1.56 (m, 2H); 1.05 (s, 3H); 0.98 (s, 3H); 0.86 (s, 3H); $^{13}C$ NMR ($CD_3CN$, $\delta_{ppm}$): 206.9 (C=O); 174.7 (C=N); 152.2, 135.3 ($CPh_{ipso}$);131.6, 125.9, 120.8, 119.3 (CPh); 58.9 (C1); 51.1 (C4); 45.1

**Table 4**
Crystallographic data for camphor imines ($OC_{10}H_{14}NY$, Fig. 2).

| | Y | |
|---|---|---|
| | 4-$CH_3C_6H_4$ | 3-$ClC_6H_4$ |
| Empirical formula | $C_{17}H_{21}NO$ | $C_{16}H_{18}ClNO$ |
| Formula weight | 255.36 | 275.78 |
| Crystal system | Orthorhombic | Orthorhombic |
| Space group | $P2_12_12_1$ | $P2_12_12_1$ |
| Unit cell dimensions | | |
| a/Å | 9.991(1) | 7.212(2) |
| b/Å | 10.386(2) | 10.921(3) |
| c/Å | 20.214(5) | 18.562(5) |
| α/deg | 90 | 90 |
| β/deg | 90 | 90 |
| γ/deg | 90 | 90 |
| Volume ($Å^{-3}$) | 1467.6(5) | 1461.9(7) |
| Z, Dcal ($g/cm^3$) | 4, 1.156 | 4, 1.253 |
| Absorption coefficient ($mm^{-1}$) | 0.071 | 0.253 |
| F(000) | 552 | 584 |
| Crystal size ($mm^3$) | 0.3 × 0.2 × 0.3 | 0.3 × 0.3 × 0.4 |
| θ range for data collection (deg) | 2.01 to 30.56 | 2.16 to 30.78 |
| Index ranges | −9 ≤h ≤9, −13 ≤k ≤14, −24 ≤l ≤28 | −10 ≤h ≤9, −15 ≤k ≤12, −26 ≤l ≤25 |
| Reflections collected/ unique | 9955/4447 [R(int) = 0.050] | 10,378/4497 [R(int) = 0.041] |
| Data/restraints/ parameters | 4447/0/176 | 4497/0/175 |
| Final R (observed) | R1 = 0.055, wR2 = 0.127 | R1 = 0.0485, w*R*2 = 0.136 |

(C7); 30.7 (C6); 24.6 (C5); 21.2, 17.4 (C9, C10); 9.3 (C8).

**[Ag($NO_3$)($OC_{10}H_{14}NC_6H_4Cl$-4)$_2$] (8)**

Elem. Anal. (%) for $AgC_{32}H_{36}N_3O_5Cl_2 \cdot H_2O$: Found.: C, 52.1; N, 5.9; H, 4.9; Calc.: C, 52.2; N, 5.7; H, 5.2. IR ($cm^{-1}$): 1745 (C=O); 1663 (C=N); 1383 ($NO_3$); $^1$H NMR ($CD_3CN$, $\delta_{ppm}$): 7.41 (d, *J* = 8.7 Hz, 2H); 6.92 (d, *J* = 8.7 Hz, 2H); 2.78 (d, *J* = 4.8 Hz, 1H); 2.12–2.03 (m, 1H); 1.92–1.87 (m, 1H); 1.64–1.55 (m, 2H); 1.04 (s, 3H); 0.98 (s, 3H); 0.84 (s, 3H); $^{13}$C NMR ($CD_3CN$, $\delta_{ppm}$): 206.9 (C=O); 174.4 (C=N); 149.3; 130.0; 123.1; 122.9; 58.9 (C1); 51.1 (C4); 45.2 (C8); 30.7 (C6); 24.6 (C5); 21.1, 17.4 (C9, C10); 9.2 (C8).

**[Ag($NO_3$)($OC_{10}H_{14}NC_6H_4F$-4)$_2$] (9)**

Elem. Anal. (%) for $AgC_{32}H_{36}N_3O_5F_2 \cdot 1.5H_2O$: Exp.: C, 53.5; N, 6.0; H, 5.0; Calc.: C, 53.7; N, 5.9; H, 5.4; IR ($cm^{-1}$): 1747 (C=O); 1651 (C=N); 1499 (Ph); 1384 ($NO_3$); $^1$H NMR ($CD_3CN$, $\delta_{ppm}$): 7.16 (t, *J* = 8.5 Hz, 2H); 6.99–6.96 (m, 2H); 2.805 (d, *J* = 4.6 Hz, 1H); 2.11–2.04 (m, 1H); 1.91–1.86 (m, 1H); 1.66–1.55 (m, 2H); 1.05 (s, 3H); 0.98 (s, 3H); 0.84 (s, 3H); $^{13}$C NMR ($CD_3CN$, $\delta_{ppm}$): 207.1 (C=O); 173.9 (C=N); 162.8, 160.4, 146.6 ($CPh_{ipso}$); 123.5, 123.4, 116.8, 116.6 (CPh); 58.8 (C1); 51.1 (C4); 45.3 (C7); 30.8 (C6); 24.6 (C5); 21.1, 17.5 (C9, C10); 9.3 (C8);

**[Ag($NO_3$)($OC_{10}H_{14}NC_6H_4CF_3$-4)$_2$] (10)**

Elem. Anal. (%) for $AgC_{34}H_{36}N_3O_5F_6$: Found.: C, 51.8; N, 5.3; H, 4.5; Calc.: C, 51.8; N, 5.3; H, 4.6; IR ($cm^{-1}$): 1751 (C=O); 1671 (C=N); 1609 (Ph); 1383 ($NO_3$); 1325, 1113 ($CF_3$); $^1$H NMR ($CD_2Cl_2$, $\delta_{ppm}$): 7.635 (d, *J* = 8.3 Hz, 2H); 7.10 (d, *J* = 8.3 Hz, 2H); 2.78 (d, *J* = 4.7 Hz, 1H); 2.19–2.04 (m, 1H); 1.97–1.82 (m, 1H); 1.72–1.48 (m, 2H); 1.08 (s, 3H); 0.98 (s, 3H); 0.85 (s, 3H); $^{13}$C NMR ($CD_2Cl_2$, $\delta_{ppm}$): 205.2 (C=O); 175.6 (C=N); 127.0 (q, *J* = 3.8 Hz); 121.7 (CPh); 58.6 (C1); 51.2 (C4); 45.1 (C7); 30.4, 24.6 (C5, C6); 21.5, 17.3 (C9, C10); 9.0 (C8); $^{19}$F NMR ($CD_3CN$, $\delta_{ppm}$): 62.54 ($CF_3$), using $BF_4^-$ ($Br_4NBF_4$) as reference ($\delta_{ppm}$ = −151.9 ppm).

**[Ag($NO_3$)($O_2SNC_{10}H_{13}NNH_2$)$_2$] (11)**

Elem. Anal. (%) for $AgC_{20}H_{30}N_7S_2O_7$: Found.: C, 37.2; N, 14.6; S, 9.7; H, 4.9; Calc.: C, 36.8; N, 15.0; S, 9.8; H, 4.6; IR ($cm^{-1}$): 3401, 3280, 3200 (N−H); 1637, 1575 (C=N); 1383 ($NO_3$); 1330 ($SO_2$ *asym*); 1158 ($SO_2$ sym). $^1$H NMR ($CD_3CN$, $\delta_{ppm}$): 7.92 (s, 0.4H (*Z*-isomer)); 7.21 (s, 1.6H (*E*-isomer)); 3.30, 3.10 (2d, *J* = 13.7 Hz, 2H); 3.045 (d, *J* = 4.1 Hz, 1H); 2.89 (s, 1H); 2.77 2.89 (s, 1H); 2.19–2.00 (m, 2H); 1.71–1.46 (m, 2H); 1.05 (s, 3H); 0.82 (s, 3H); $^{13}$C NMR ($CD_3CN$, $\delta_{ppm}$): 186.4 (C2); 141.8 (C3); 64.5 (C1); 50.0 (C8); 48.5 (C7); 47.4 (C4); 30.4, 23.9 (C5, C6); 19.5, 18.6 (C9, C10).

#### 4.1.3. Antibacterial activity determinations

The Gram-positive *Staphylococcus aureus Newman*, and the Gram-negative *Pseudomonas aeruginosa* 477, *Escherichia coli* ATCC 25922, and *Burkholderia contaminans* IST408 were used in this work. When in use, bacteria were maintained in Lennox Broth (LB) solid medium (Sigma-Aldrich, St. Louis, USA), otherwise cultures were kept frozen at −80 °C. Minimum Inhibitory Concentration (MIC) of camphorimine Ag(I) complexes were assessed by microdilution assays in Muller-Hinton broth (MH) (Sigma-Aldrich, St. Louis, USA) using at least 3 independent experiments carried out in duplicate, as previously described [13,16]. For these purposes, overnight bacterial cultures grown at 37 °C in MH with orbital shaking (250 rev.$min^{-1}$) were diluted with fresh MH medium to a final optical density, measured at 640 nm ($OD_{640}$) of 0.02, in a Hitachi U-2000 UV/Vis spectrophotometer. 100 µL aliquots of cell suspensions were mixed in 96-wells polystyrene plates with 100 µL of fresh MH containing previously serially diluted (1:2) camphorimine Ag (I) complexes from stock solutions. The $OD_{640}$ of the cultures were measured after 24 h of incubation at 37 °C using a SpectrostarNano microplate reader (BMG Labtech, Germany). The MIC values were estimated by fitting the $OD_{640}$ mean values with a Gompertz modified equation [13].

#### 4.1.4. Computational details

The optimization of the structures and the molecular geometry of the complexes were carried out by DFT calculations using GAMESS-US [30], version R3 with a CAMB3LYP functional [31], and 65% HF exact exchange at long range and 19% at short range, using a SBKJC basis set.

#### 4.1.5. X-ray diffraction

X-ray data for camphor imine ligands $OC_{10}H_{14}NY$ (Y = 4-$CH_3C_6H_4$ and Y = 3-$ClC_6H_4$) was collected at room temperature using a Bruker AXS-KAPPA APEX II area detector apparatus equipped with a graphite-monochromated Mo Kα (λ = 0.71073 Å) and were corrected for Lorentz polarization and, empirically, for absorption effects. The structures were solved by direct methods using SHELX97 [32] and refined by full matrix least squares against $F^2$ using SHELX97 all included in the suite of programs WinGX v1.70.01 for Windows [33]. The non-hydrogen atoms were refined anisotropically and the H atoms were inserted in idealized positions and allowed to refine riding on the parent atom. Crystal data and refinement parameters are summarized in Table 4. Illustrations of the molecular structures were made with ORTEP3 [34].

## Acknowledgements

Financial support by FCT-Fundação para a Ciência e a Tecnologia through projects ID/QUI/00100/2019, UID/BIO/04565/2019, Grant BL-CQE/2018-013 and the NMR Network (IST-UTL Node) for facilities are gratefully acknowledged.

## Appendix A. Supplementary data

Cambridge Crystallographic Data Centre (CCDC 1915955-1915956) contains the supplementary crystallographic data for this article. The X-ray data can be obtained free of charge via www.ccdc.cam.ac.uk/conts/retrieving.html (or from the CCDC, 12, Union Road, Cambridge CB2 1EZ, UK; fax: þ44 1223 336033 or deposit@ccdc.cam.ac.uk).

Supplementary Information – Relevant NMR data is provided for complexes (36 spectra). Supplementary data to this article can be found online at https://doi.org/10.1016/j.jinorgbio.2019.110791.

## References


[1] S. Silver, FEMS Microbiol. Rev. 27 (2003) 341–353.
[2] L.J. Wilkinson, R.J. White, J.K. Chipman, J. Wound Care 20 (2011) 543–549.
[3] P. Singha, J. Locklin, H. Handa, Acta Biomater. 50 (2017) 20–40.
[4] W.-G. Kwak, M.H. Oh, S.-Y. Son, M.-S. Gong, Macromol. Res. 23 (6) (2015) 509–517.
[5] W. Sim, R.T. Barnard, M.A.T. Blaskovich, Z.M. Ziora, Antibiotics 7 (2018) 93.
[6] M. Muller, Antimicrob. Agents Chemother. (2018), https://doi.org/10.1128/AAC.00672-18 May 14. pii: AAC.00672-18.
[7] K. Mijnendonckx, N. Leys, J. Mahillon, S. Silver, R. Van Houdt, Biometals 26 (4) (2013) 609–621, https://doi.org/10.1007/s10534-013-9645-z.
[8] X. Yan, B. He, L. Liu, G. Qu, J. Shi, L. Hu, G. Jiang, Metallomics 10 (4) (2018) 557–564.
[9] M.I. Azocar, G. Gomez, P. Levin, M. Paez, H. Muñoz, N. Dinamarca, J. Coord. Chem. 67 (2014) 3840–3853.
[10] F. Long, C.-C. Su, M.T. Zimmermann, S.E. Boyken, K.R. Rajashankar, R.L. Jernigan, E.W. Yu, Nature 467 (2010) 484–488.
[11] J.M.S. Cardoso, I. Correia, A.M. Galvão, F. Marques, M.F.N.N. Carvalho, J. Inorg. Biochem. 166 (2017) 55–63.
[12] X. Liang, S. Luan, Z. Yin, M. He, C. He, L. Yin, Y. Zou, Z. Yuan, L. Li, X. Song, C. Lv, W. Zhang, Eur. J. Med. Chem. 157 (2018) 62–80.
[13] F. Barras, L. Aussel, B. Ezraty, Antibiotics 7 (2018) 79.
[14] J.M.S. Cardoso, S.I. Guerreiro, A. Lourenço, M.M. Alves, M.F. Montemor, N.P. Mira, J.H. Leitão, M.F.N.N. Carvalho, PLoS One (2017) 1–15 May 9.
[15] J.H. Leitão, S.A. Sousa, S.A. Leite, M.F.N.N. Carvalho, Antibiotics 7 (3) (2018) 65.
[16] J.M.S. Cardoso, A.M. Galvão, S.I. Guerreiro, J.H. Leitão, A.C. Suarez, M.F.N.N. Carvalho, Dalton Trans. 45 (2016) 7114–7123.
[17] M.F.N.N. Carvalho, M.T. Duarte, T.A. Fernandes, A.M. Galvão, A.M. Botelho do Rego, Inorg. Chem. 49 (2010) 10330–10337.
[18] A.S.D. Ferreira, M.F.N.N. Carvalho, A.M. Galvão, L.F. Veiros, Inorg. Chim. Acta 395 (2013) 169–175.
[19] S.M. Soliman, Y.N. Mabkhot, A. Barakat, H.A. Ghabbour, J. Coord. Chem. 70 (2017) 1339–1356.
[20] M.F.N.N. Carvalho, L.M.G. Costa, A.J.L. Pombeiro, A. Schier, W. Scherer, S.K. Harbi, U. Verfürth, R. Herrmann, Inorg. Chem. 33 (1994) 6270–6277.
[21] S. Medici, M. Peana, G. Crisponi, V.M. Nurchi, J.I. Lachowicz, M. Remelli, M.A. Zoroddu, Coord. Chem. Rev. 327–328 (2016) 349–359.
[22] I. Ghai, S. Ghai, Infect. Drug Resist. 11 (2018) 523–530.
[23] S.A. Sousa, J.R. Feliciano, T. Pita, S.I. Guerreiro, J.H. Leitão, Genes 8 (2017) 43.
[24] A. Lamut, L.M. Peterlin, D. Kikelj, T. Tomašič, Med. Res. Rev. (2019) 1–45.
[25] M.F.N.N. Carvalho, A.C. Consiglieri, M.T. Duarte, A.M. Galvão, A.J.L. Pombeiro, R. Herrmann, Inorg.Chem. 32 (1993) 5160.
[26] W.L.F. Armarego, C.L.L. Chai, Purification of Laboratory Chemicals, sixth ed., Elsevier Inc, Oxford, 2008.
[27] M.0. Forster, H. Spinner, J. Chem. Soc. 101 (1912) 1340.
[28] J.D. White, D.J. Wardrop, K.F. Sundermann, Org. Synth. Coll. 10 (2004) 204.
[29] S.D. Denmark, I. Rivera, J. Organomet. Chem. 59 (1994) 6887.
[30] M.W. Schmidt, K.K. Baldridge, J.A. Boatz, S.T. Elbert, M.S. Gordon, J.H. Jensen, S. Koseki, N. Matsunaga, K.A. Nguyen, S. Su, T.L. Windus, M. Dupuis, J.A. Montgomery, J. Comput. Chem. 14 (1993) 1347–1363.
[31] T. Yanai, D. Tew, N. Handy, Chem. Phys. Lett. 393 (2004) 51–57.
[32] G.M. Sheldrick, SHELX-97- Programs for Crystal Structure Analysis (Release 97–2), Institüt für Anorganische Chemie der Universität, Tammanstrasse 4, D-3400 Göttingen, Germany, 1998.
[33] L.J. Farrugia, WINGX J. Appl. Crystallogr. 32 (1999) 837.
[34] L.J. Farrugia, J. Appl. Crystallogr. 30 (1997) 565.